Environmental Science & Technology

pubs.acs.org/est

Article

# Exogenous Electroactive Microbes Regulate Soil Geochemical Properties and Microbial Communities by Enhancing the Reduction and Transformation of Fe(III) Minerals

Xiaolin Zhang,[⊥] Yuxia Liu,[⊥] Qixing Zhou,* Yuge Bai, Ruixiang Li, Tian Li,* Jintian Li, Daniel S. Alessi, and Kurt O. Konhauser

Cite This: *Environ. Sci. Technol.* 2023, 57, 7743−7752

Read Online

ACCESS | Metrics & More | Article Recommendations | Supporting Information

**ABSTRACT:** Electroactive microbes can conduct extracellular electron transfer and have the potential to be applied as a bioresource to regulate soil geochemical properties and microbial communities. In this study, we incubated Fe-limited and Fe-enriched farmland soil together with electroactive microbes for 30 days; both soils were incubated with electroactive microbes and a common iron mineral, ferrihydrite. Our results indicated that the exogenous electroactive microbes decreased soil pH, total organic carbon (TOC), and total nitrogen (TN) but increased soil conductivity and promoted Fe(III) reduction. The addition of electroactive microbes also changed the soil microbial community from *Firmicutes*-dominated to *Proteobacteria*-dominated. Moreover, the total number of detected microbial species in the soil decreased from over 700 to less than 500. Importantly, the coexistence of N-transforming bacteria, Fe(III)-reducing bacteria and methanogens was also observed with the addition of electroactive microbes in Fe-rich soil, indicating the accelerated interspecies electron transfer of functional microflora.

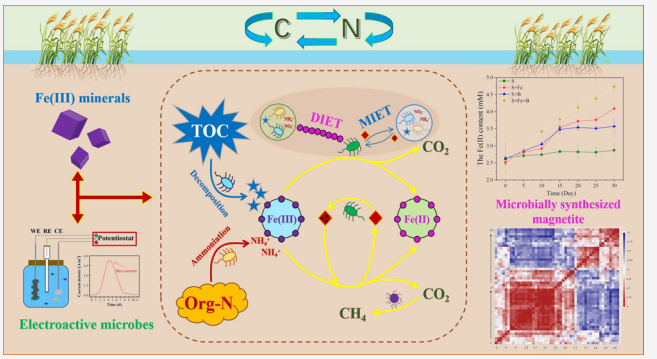


**KEYWORDS:** *geochemical process, exogenous $Fe(OH)_3$, electroactive microbes, microbial communities, electron transfer*



## INTRODUCTION

Electroactive microbes gain energy from either accepting electrons or donating electrons to electrodes.[1] Electron transfer occurs in three primary ways: (1) direct contact of microbial outer membrane cytochromes to the electrodes; (2) microbes produce conductive extensions, such as pili, to reach the electrode; and (3) microbes excrete redox-active compounds, such as flavins, as electron shuttles between themselves and the electrode.[2−5] Due to their ability to generate electrical current without the addition of any artificial mediator, these electroactive microbes have attracted increasing attention in the past decade.[6−8] For example, studies have shown that electroactive microbes can contribute to electricity production,[9] wastewater treatment,[10] and the clean production of hydrogen gas ($H_2$)/methane ($CH_4$).[11] To date, one of the best studied electroactive bacteria is *Geobacter* sp.,[1,10] which is also widely known for its ability to reduce iron (Fe)(III) minerals.[12,13]

As an abundant and reactive metallic element in the earth's crust, Fe is widely present in soils and sediments in the form of Fe(III) minerals.[14] Dissimilatory Fe(III)-mineral reduction is an important biogeochemical redox process that occurs in diverse anoxic environments, such as soils and sediments.[12] Previous studies have showed that the reduction of Fe(III) minerals can lead to the subsequent formation of Fe(II)-bearing secondary minerals including magnetite, siderite, vivianite, and green rust.[15,16] These secondary minerals can then be reoxidized back to Fe(III) either chemically or by Fe(II)-oxidizing microbes.[17] Because of their large surface areas, Fe minerals are strong sorbents for soil nutrients, organic compounds, and contaminants.[18] Therefore, the redox cycle of Fe has a significant impact on other geological and environmental processes,[12,19] the remobilization of toxic metals,[20,21] and the degradation of organic pollutants.[22,23]

As the research on electroactive microbes continues, these microbes are likely to be used in a wide range of industrial applications in the near future. However, to date, it remains unknown how these microbes, especially when they are enriched, influence soil geochemical properties and biogeochemical processes once introduced into soil ecosystems. For

Received: January 16, 2023
Revised: March 23, 2023
Accepted: April 29, 2023
Published: May 12, 2023




https://doi.org/10.1021/acs.est.3c00407
*Environ. Sci. Technol.* 2023, 57, 7743−7752

instance, once introduced into iron-containing soils, *Geobacter* may fundamentally change the environment by promoting the reduction of Fe(III) minerals.[24] Therefore, in this study, we incubated enriched electroactive microbes in soil to investigate their effects on the soil microbial community and biogeochemical cycling of carbon (C) and nitrogen (N). In addition, we added a common Fe(III)-bearing mineral, ferrihydrite, to soil systems to determine the effects of abundant or limited Fe(III) on changes in soil geochemical properties, microbial community compositions, and elemental cycling caused by electroactive microbes. By conducting these experiments, we aim to answer the following questions: (1) How do soil geochemical properties change with the addition of enriched electroactive microbes; (2) How do soil microbial community compositions and function vary with enriched electroactive microbes; and (3) How does the enrichment of electroactive microbes in soil affect the element cycling of C and N by promoting Fe(III)-mineral reduction?

## MATERIAL AND METHODS

**Soil Treatment and Analysis.** Topsoil samples (0−15 cm) were collected from a farmland in Jinnan District (38.99 N, 117.33 E) in the Tianjin Municipality of China. After removing stones, branches, and other debris, the soil samples were air-dried under ventilated conditions. Afterward, the dried soil samples were passed through a 2 mm sieve and preserved at −4 °C until further use. Here, topsoil samples were selected as experimental objects because they contain more abundant microbial resources (including electroactive microbes) due to the input of organics and has a higher Fe(III) content compared to the anaerobic layer. The iron minerals identified from the original soil were mainly Schafarzikite ($FeSbO_4$) and Neptunite ($KNa_2LiFe_2Ti_2Si_8O_{24}$) by X-ray diffraction (XRD) testing with gallery matching (Figure S1).

Several geochemical characteristics of soil samples were determined. The soil conductivity and pH were measured using conductivity and pH meters (Mettler Toledo, Shanghai, China) at a soil to water ratio of 1:5 (*w*/*v*). Total organic carbon (TOC) of the soil sample was determined using an organic carbon analyzer (Multi N/C 3100, Jena, Germany) by combusting 10 mg of soil at 1200 °C. The inorganic C of the soil samples was removed prior to the TOC analysis by incubating with 1 M hydrochloride acid (HCl) until no bubble formation could be observed. The ammonium nitrogen ($NH_4^+$-N) concentration in the soil samples was determined by the indophenol blue colorimetric assay,[25] measured at 625 nm wavelength in 96-well plates (SPARK 10 M, TECAN Ltd., Männedorf, Switzerland) with UV−vis spectroscopy (T6-1650F, Persee Instrument Co. Ltd., Beijing, China). The nitrate nitrogen ($NO_3^-$-N) was also analyzed with the UV−vis spectroscope at a wavelength of 220 nm.

**Cultivation of Electroactive Microbes from the Soil.** The electroactive microbes were isolated from the soil leachate by adding 2 mL of distilled water per gram (g) of soil. To start the enrichment, the 200 mL soil leachate was made anoxic by being flushed with $N_2/CO_2$ (4:1) for 30 min. Then, the anoxic leachate was added into an anoxic three-electrode bioelectrochemical system with a constant voltage of 0.2 V (vs Ag/AgCl) (Figure 1).[26] The pH of the system was maintained at around 7.0 with a 50 mM phosphate buffer solution. The electrical current created in the system was monitored by a multichannel potentiostat at 100 s intervals, and once the current became lower than $10^{-6}$ mA, we considered that one

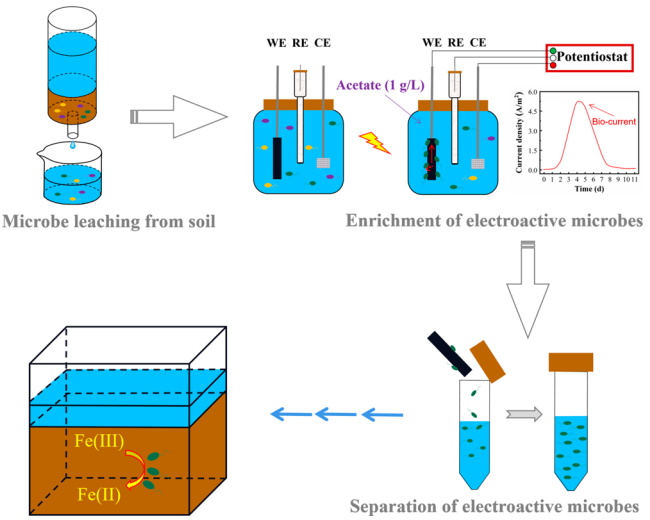


**Figure 1.** Steps for enrichment and separation of electroactive microbes from soil conducted in this work. The graphite rod working electrode (WE), platinum sheet counter electrode (CE), and Ag/AgCl reference electrode (RE) were applied in a three-electrode bioelectrochemical system.

enrichment cycle was completed. Afterward, 0.012 M sodium acetate was added into the enrichment system to start the next cycle. After two enrichment cycles, electroactive microbes were scraped from the electrode and dispersed in distilled water in an anaerobic environment. The process for enrichment and separation of electroactive microbes from soil is shown in Figure 1. A portion of the enriched culture was continuously batch-fed and stored in the anoxic three-electrode bioelectrochemical system as mentioned above and the biofilm samples collected from the anode were stored in glycerol-sealed sterile tubes for durable cryopreservation and identification of the microbial passage stability. The typical electroactive bacteria, *Geobacter*, has long dominated the microbial community structure according to the microbial composition of the cultures enriched from the three-electrode bioelectrochemical system (Figure S2). Compared with the cultured pure electroactive bacteria, the electroactive microbes enriched from the soil leachate have higher adaptability to the original habitat and the operation of enrichment is convenient and conducive to large-scale application.

**Soil Incubation Experiment Setup.** The electroactive microbes were amended into soil samples immediately following the completion of the enrichment process to avoid cell lysis. Before being introduced into the soil, the density of the electroactive microbes should reach an $OD_{600}$ value of 0.8 to ensure the enrichment of the electroactive bacterium. In order to test the effects of electroactive microbes on the soil properties and elemental cycling with either abundant or limited Fe(III) in the soil, we conducted four groups of experiments: (1) an experiment with 1 kg of soil, 100 mM ferrihydrite and 150 mL of electroactive microbes cell suspension, and this experiment was called S+Fe+B; (2) an experiment with 1 kg of soil and 100 mM ferrihydrite only, which was labeled as S+Fe; (3) an experiment with 1 kg soil and 150 mL of electroactive microbes cell suspension, and this set of experiment was marked as S+B; and (4) a control experiment with only 1 kg of soil, which was labeled as S. For all experiments, unsterilized soil was used. The ferrihydrite used in all experiments was synthesized by dissolving


https://doi.org/10.1021/acs.est.3c00407
Environ. Sci. Technol. 2023, 57, 7743−7752

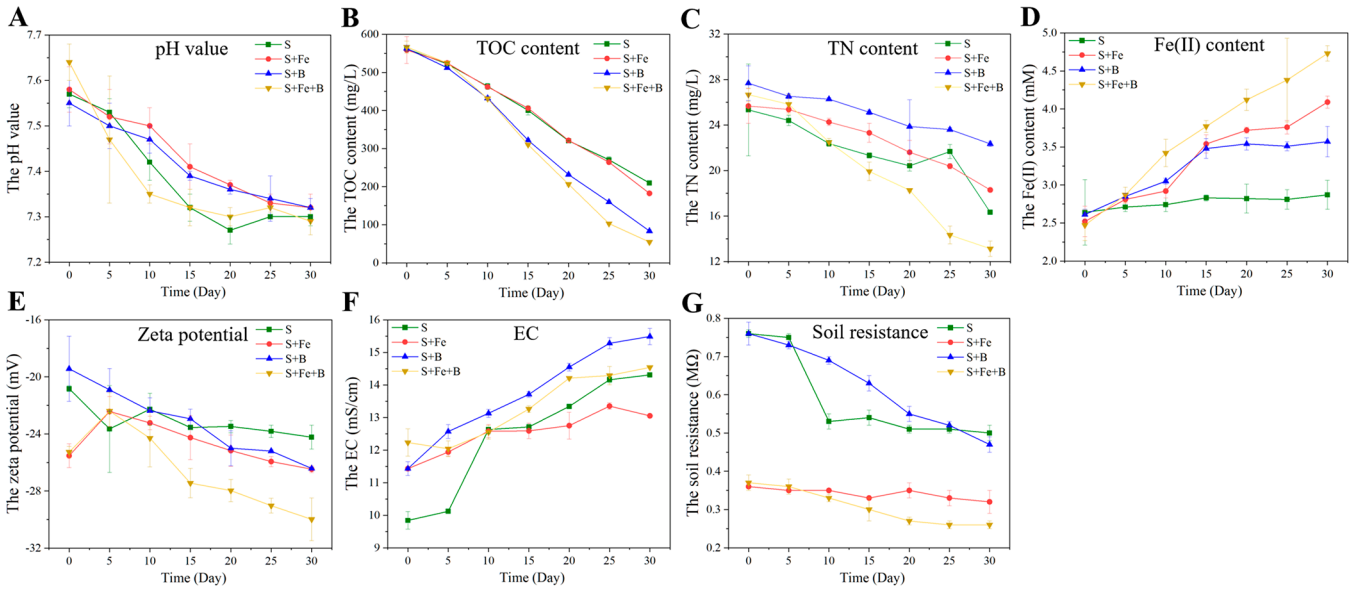


**Figure 2.** Changes of (A) pH, (B) total organic carbon (TOC), (C) total nitrogen, (D) Fe(II) production, (E) $\zeta$ potential, (F) electrical conductivity (EC), and (G) soil resistance with and without microbially driven magnetite production from 0 day to 30 day. The S with the green color represents the group including natural soil only; the S+Fe with the red color represents the group including both natural soil and 100 mM $Fe(OH)_3$; the S+B with the blue color represents the group including both natural soil and 150 mL electroactive microbes; and the S+Fe+B with the yellow color represents the group including natural soil, 100 mM $Fe(OH)_3$, and 150 mL of electroactive microbes.

$Fe(NO_3)_3{\cdot}9H_2O$ into distilled water and neutralizing the pH to 7−8 with 4 M NaOH.[27] One gram of sodium acetate per kg of soil was added as the electron donor to maintain the activity of electroactive microbes in the start-up phase, and distilled water was added to the surface of the soil to form a 2 cm water-seal layer, therefore keeping the anoxic conditions in the experiments. Triplicates were set up for each group of experiment. The experimental setups were incubated up to one month, and the samples were collected from the soil at a depth of 4−6 cm, where anerobic conditions were achieved, every 5 days to evaluate changes in soil properties. And, the microbial community compositions of the different treatment groups were analyzed on day 30.

**Fe(II) Concentration Measurements and Characterization.** The Fe(II) concentration and the Fe mineral phases were analyzed in the soil samples taken from the column incubation experiments. Before the concentration measurement, all soil samples were weighted and digested with 25% HCl. After centrifugation to remove the particles, the Fe(II) concentration in the supernatant was measured by the phenanthroline spectrophotometric method on a 96-microplate reader (SPARK 10 M, TECAN Ltd., Männedorf, Switzerland) at a wavelength of 510 nm.[28] The Fe mineral phases in the soil of different groups after the incubation experiment were characterized by scanning electron microscopy (SEM), Fourier transform infrared spectroscopy (FTIR), and Raman spectroscopy. Moreover, to identify the microbially synthesized magnetite in S+Fe+B, it was extracted from the soil system using neodymium magnet and characterized by X-ray diffraction (XRD), FTIR, and Raman spectroscopy. See Text S1 of the Supporting Information (SI) for the operation details of these three methods.

**Geochemical Characterization of Soil Samples.** The soil samples from the incubation experiments were characterized for pH, soil conductivity, TOC, $\zeta$ potential, and soil resistance. The details for the pH, conductivity and TOC analyses can be found in the section above. For the $\zeta$ potential measurement, 1 g of soil sample was ground in a mortar pestle to a particle size <10 $\mu$m. Following, sodium chloride (NaCl) (170 mM) was added to the samples to buffer the ionic strength to 20 $\mu S\ cm^{-1}$. NaOH (0.5 M) and 0.1 M HCl were added dropwise to adjust pH values to a final pH of 7.57. After this, the $\zeta$ potentials of the soil samples were measured with a $\zeta$ potential analyzer (JS94K, Powereach). The resistance levels of the soil samples were directly measured by a multimeter (DL334002, Deli Ltd., Ningbo, China).

**Soil Microbial Community Analysis.** Soil samples for the microbial community analysis were collected with a sterile spoon into sterilized centrifuge tubes. DNA was extracted using a Soil Genomic DNA kit (CW2091S, ComWin Biotech Co., Ltd., Beijing, China) according to manufacturer protocols. The primers 338F (5′-ACTCCTACGGGAGGCAGCAG-3′) and 806R (5′-GGACTACHVGGGTWTCTAAT-3′) were applied to amplify the V3−V4 region of bacterial 16S rRNA. The PCR products were recovered by an AxyPrep DNA Gel Recovery kit (AXYGEN) and then eluted by Tris-HCl. For each sample, the DNA extraction and amplification were repeated three times. A mixture of these three extractions was used for the detection of the purity of the PCR products by 2% agarose gel electrophoresis. The amplicons were subsequently sent to Majorbio (Shanghai, China) for MiSeq Illumina sequencing, and the data were analyzed through the platform provided by Majorbio (www.majorbio.com). A QuantiFluor-ST blue fluorescence quantitative system (TBS-380, Promega) was applied for the quantification of PCR products and the construction of genomic library. The MiSeq (PE300, Illumina) was used to perform library sequencing on a paired terminal platform by Majorbio (Shanghai, China). The PE reads obtained by Illumina sequencing were spliced (https://ccb.jhu.edu/software/FLASH/index.shtml) according to the overlap relationship and the sequence quality was controlled and filtered. The software Uparse (version 7.0.1090, http://drive5.com/uparse/) was used for OTU clustering of nonrepetitive sequences according to 97% similarity. The RDP classifier


https://doi.org/10.1021/acs.est.3c00407
Environ. Sci. Technol. 2023, 57, 7743−7752

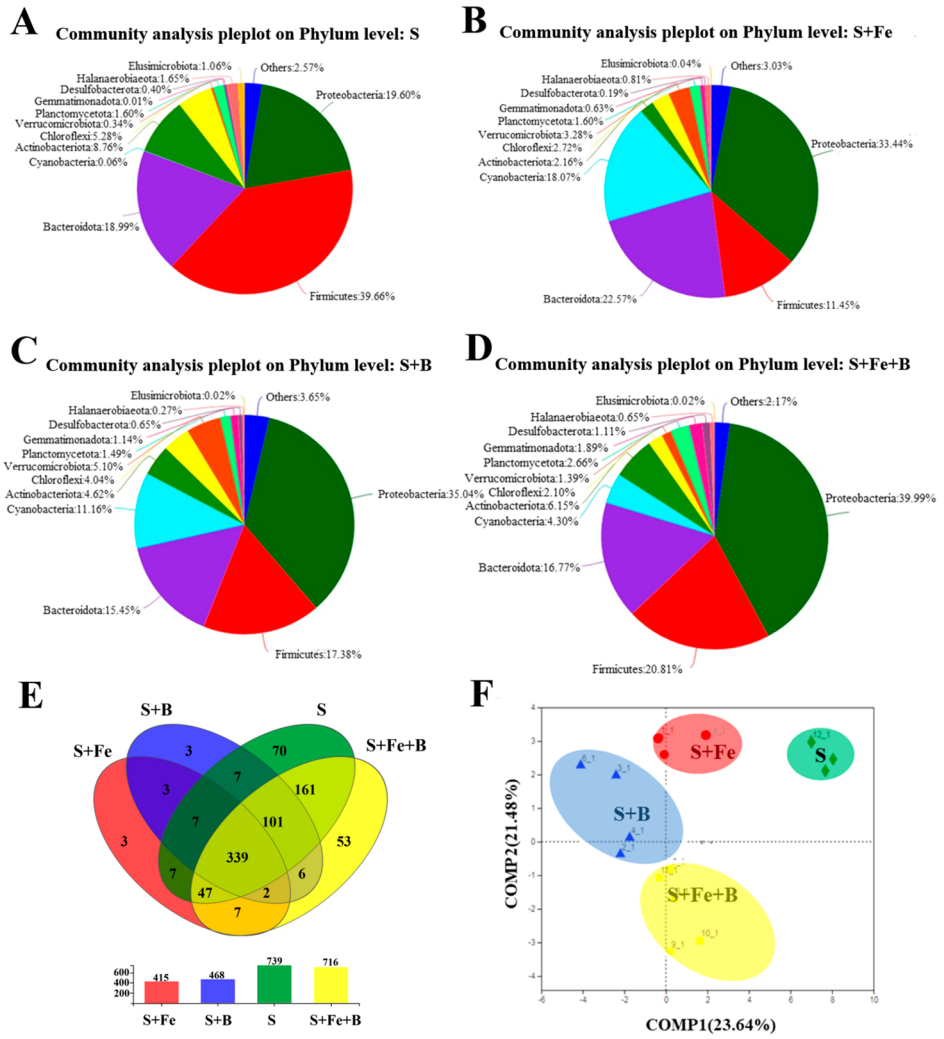


**Figure 3.** Microbial community analyses at the phylum level in groups (A) S, (B) S+Fe, (C) S+B, and (D) S+Fe+B, respectively, (E) Venn diagram of the microbes at the phylum level in different groups, and (F) PLS-DA at the phylum level in different groups. A–D represent the groups of S, S +Fe, S+B, and S+Fe+B, respectively, which were analyzed by R program. For E and F, the region in green color represents the group of S, while the region in red color represents the group of S+Fe, the region in blue color represents the group of S+B, and the region in yellow color represents the group of S+Fe+B.

Bayesian algorithm was applied for species taxonomic analysis of OTU representative sequences with 97% similarity level based on the Silva database (Release,138 http://www.arb-silva.de). The raw data reads were deposited in the NCBI GenBank with an accession number of PRJNA942223. The visual analysis of microbial sequences is presented in Text S2 of the SI section.

**Statistical Analysis.** Statistical analyses in this study were performed using one-way analysis of variance (ANOVA) followed by the least significant difference (LSD). The LSD results are reported only if the one-way ANOVA test showed a significant effect.[29] The statistical analysis was represented by $p$ in this study. When $p$ was between 0.01 and 0.05, the data were marked as *, indicating significant difference. When $p$ was below 0.01, the data were marked as **, indicating even greater significant difference.

## RESULTS AND DISCUSSION

**Enhanced Fe(III) Mineral Reduction by Electroactive Microbes Changes the Soil Geochemical Properties.** In Figure 2, the pH, conductivity, resistance, TOC, $\zeta$ potential, and the Fe(II) concentrations of soil sampled from all four experimental setups are plotted against the incubation time (30 d). As shown in Figure 2A, the pH in all experiments decreased over time, generally from around 7.6 to around 7.3 over 30 days of incubation. The decrease of pH likely results from the accumulation of small molecular organic acids during the mineralization of soil organic matter under water-locked (anoxic) conditions in our experiments.[30,31] The degradation of soil organic matter also decreased TOC (Figure 2B) during the incubation. As shown in Figure 2B, while the experiment with the addition of ferrihydrite (S+Fe) showed a similar extent of TOC decrease (~550 to ~250 mg C $L^{-1}$) to that of the control experiment (S), the addition of electroactive microbes (S+B) significantly decreased the TOC from around 550 to 100 mg C $L^{-1}$. Moreover, the experiment with additional ferrihydrite (S+Fe+B), representing a Fe-rich soil, showed an even greater TOC decrease from around 550 to about 50 mg C $L^{-1}$. We suggest that more TOC consumption in the experiments with electroactive microbes was due to the ability of these microbes to directly facilitate extracellular electron transfer during the metabolism of small molecular


https://doi.org/10.1021/acs.est.3c00407
Environ. Sci. Technol. 2023, 57, 7743−7752

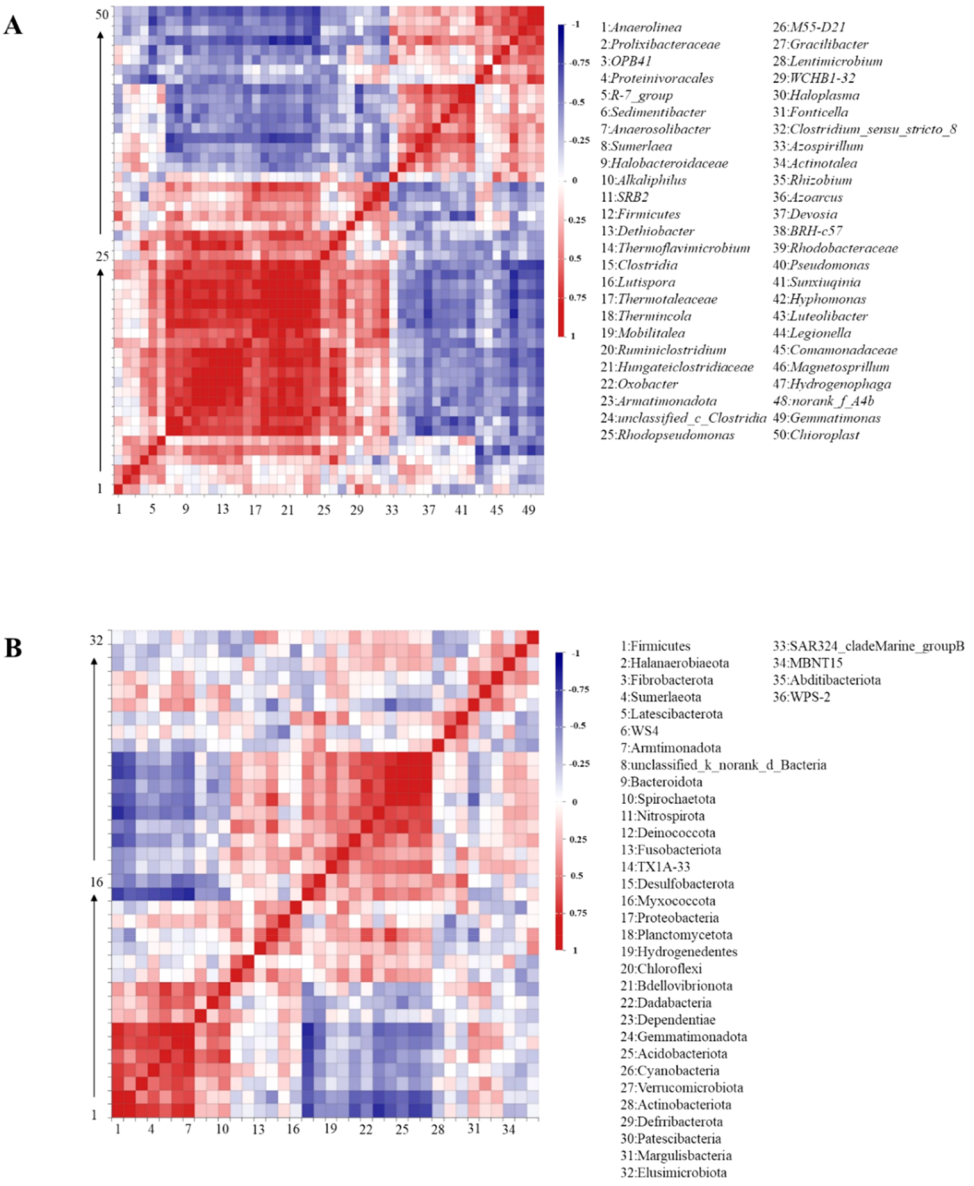


**Figure 4.** Correlation matrix between microbes at the (A) genus level and (B) phylum level for group S+Fe+B (Spearman test). Red regions represent positive correlation between two microbes and the correlation increases with the intensity of the color. Blue regions represent negative correlation between two microbes and the correlation increases with the intensity of the color. The correlation coefficient analysis is based on OTU numbers of microbes and determined using a bivariate model (SPSS 23.0).

organics and stimulate alternative microbial respiration pathways in the soil by the expanded pool of electron acceptors (e.g., Fe(III), nitrate, sulfate, and dissolved/granular organics).[32] In particular, the rate of organic matter degradation was significantly higher in the S+Fe+B treatment than in the S+B treatment, after 15 days of incubation ($p < 0.05$). While no significant difference in TOC reduction was observed between S+Fe+B and S+B in the early stage, which could be attributed to the slow colonization of functional microflora.

The TN consumption of 19−51% was also observed in all treatment groups along with the TOC utilization during the 30 day incubation (Figure 2C). Electroactive bacteria have been reported to stimulate the ammoniation process of nitrogenous organics, in which more $NH_4^+$ is released, resulting in a significantly higher TN content in S+B than S by 2−6 mg N $L^{-1}$.[33] While the simultaneous introduction of electroactive microbes and Fe(III) minerals consumed the highest TN content (14 mg N $L^{-1}$) in S+Fe+B by enhancing the dissimilatory iron reduction within 30 days, it was noted that TN consumption in S+Fe was slower relative to S, possibly due to the stress effect of excess iron on cells.[34]

As demonstrated in previous studies,[1,35] electroactive microbes, such as the Fe(III)-reducing bacteria *Geobacter*, can degrade organic matter either by attaching to ferric iron minerals and then directly using electrons from organic matter decomposition to reduce those ferric iron minerals, or by conducting extracellular electron transfer *via* soluble intermediates to ferric iron minerals not in intimate association with the heterotrophs. The latter process is commonly defined as "electron shuttling". Due to the low solubility of Fe(III) minerals under most environmental pH conditions, the organic matter electron shuttling process can help Fe(III)-reducing bacteria to reduce Fe(III) minerals that are separated by distance and significantly enhance the rate and extent of


https://doi.org/10.1021/acs.est.3c00407
Environ. Sci. Technol. 2023, 57, 7743−7752

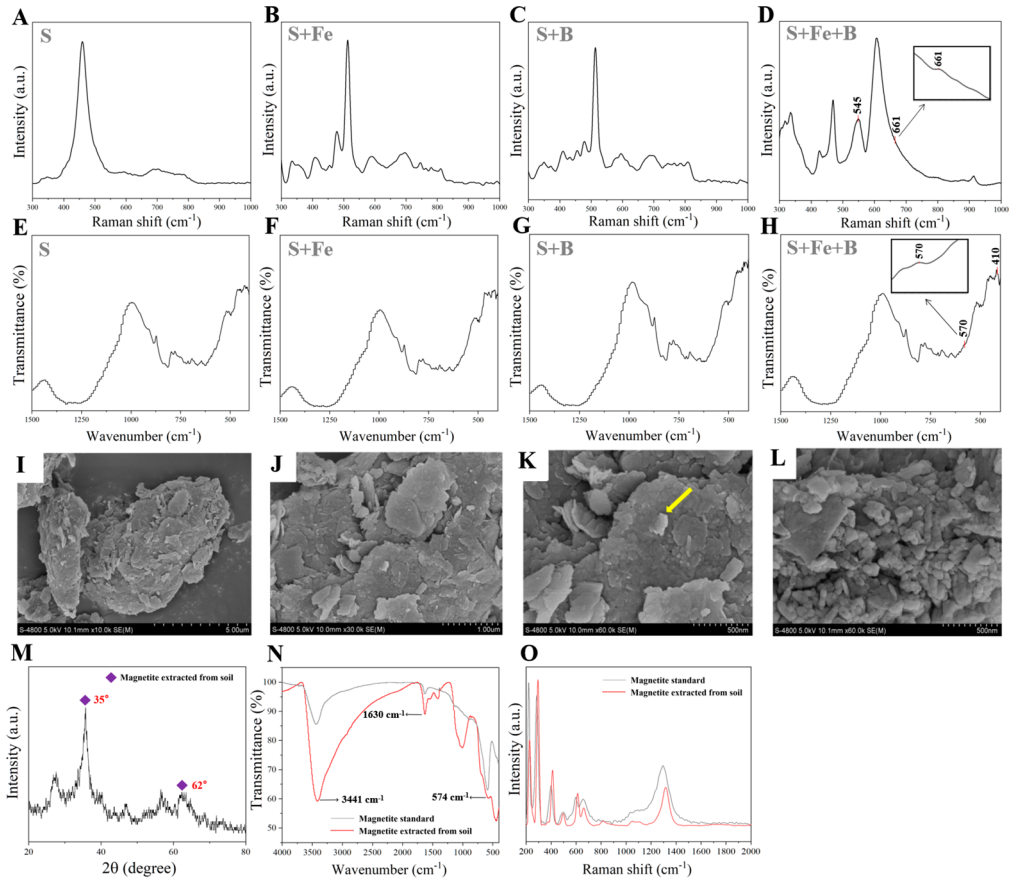


**Figure 5.** (A–D) Raman spectrum analysis and (E–H) FTIR analysis of the soil in S, S+Fe, S+B, and S+Fe+B groups. The peaks at 661 and 538 $cm^{-1}$ of Raman spectrum were regarded as characteristic A1g and T2g modes in magnetite,[55] which were also seen for the S+Fe+B group (D). The FTIR spectrum of S+Fe+B (H) displayed two peaks at 570 and 410 $cm^{-1}$, which are characteristic absorption peaks of magnetite.[56] SEM analysis of (I–K) group S+Fe+B and (L) group S. SEM in I was taken under 10.0k, while J was taken under 30.0k and K and L were taken under 60.0k. The crystalline mineral is indicated by the yellow arrow in K. (M) XRD spectra of the microbially synthesized magnetite extracted from the soil system in S+Fe+B. The two characteristic peaks at $2\theta = 35°$ and $2\theta = 62°$ were identified from magnetite.[57] (N) FTIR analysis of the magnetite standard (gray line) and microbially synthesized magnetite (red line) extracted from the soil system in S+Fe+B. The peaks in the magnetite standard (at 3441, 1630, and 574 $cm^{-1}$) are all found in microbially synthesized magnetite. (O) Raman spectroscopy of the magnetite standard (gray line) and microbially synthesized magnetite (red line) extracted from the soil system in S+Fe+B. The magnetite standard and microbially synthesized magnetite exhibit identical peak shapes.

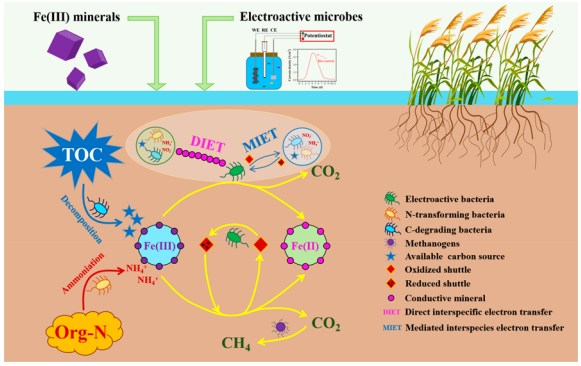


**Figure 6.** Conceptual model of C and N turnover accelerated by electroactive microbial-mediated Fe(III) reduction in the soil.

Fe(III)-mineral reduction.[5] This process can also explain the increase of Fe(II) concentration in the experiments amended with electroactive microbes (S+B and S+Fe+B), as shown in Figure 2D. Theoretically, the addition of Fe(III)-reducing bacteria, such as *Geobacter*, naturally enhances the reduction of Fe(III)-minerals in soil. However, in our experiments, the solubility of Fe(III) minerals in the soil at pH of 7–8 was very limited. Therefore, the increased Fe(II) concentration observed in the experiments with electroactive microbes (S+B and S+Fe+B) are likely attributable to enhanced Fe(III)-mineral reduction by soil organic matter electron shuttling processes. Additionally, a significant increase in Fe(II) content has also been observed in S+Fe relative to control group (S), which may be due to the exogenous Fe(III) minerals driving the activity of soil native electroactive bacteria to perform the Fe(III) reduction process. Noticeably, the extent of ferrihydrite reduction was much lower than in previous studies,[3,5] since the 30-day Fe(II) yield was only about 4.7 ± 0.1 mM with the addition of both electroactive microbes and 100 mM ferrihydrite. This may be attributed to decreases in the number and activity of electroactive microbes due to the impurity of the inoculation source contained various electroactive microbes and the competition it will generate between indigenous bacteria.

Degradation of organic matter can also explain the more negative $\zeta$ potential shown in the experiments with the addition of electroactive microbes (i.e., S+B and S+Fe+B) in Figure 2E. In these cases, more organic matter is broken down


https://doi.org/10.1021/acs.est.3c00407
Environ. Sci. Technol. 2023, 57, 7743–7752

to inorganic carbon (i.e., $CO_2$ or $HCO_3^-$ in solution) together with the release of cytoplasm and accumulation of small molecular organic acids;[30,31,36] therefore, a more negative surface charge was observed in the experiments containing electroactive microbes, compared to experiments without the addition of these microbes. Additionally, the more negative electric potential may increase the repulsive force between soil colloids which usually negatively charged, resulting in a more stable soil structure.[37]

The conductivity of the soil during the incubation, shown in Figure 2F, increased in all experimental setups except the one with the addition of ferrihydrite (S+Fe). The increase in conductivity in the control experiment with only soil (S) might be due to increased mobile soil electrolyte (e.g., $NH_4^+$) released from the degradation of organic matter during the anoxic incubation.[30] The conductivity of soil also increased significantly in the experiment with electroactive microbes added (S+B), a predictable trend due to the naturally high conductivity of these microbes.[38] In comparison to the experiment amended with only electroactive microbes, the soil conductivity increased less in the experiment with both ferrihydrite and electroactive microbes (S+Fe+B). This may reflect the adsorption of microbes onto the surface of ferrihydrite, which resulted in decreased mobility of the microbes and limited the rate of electron transfer. The affinity of ferrihydrite to electroactive microbes has been observed in previous work.[39] Soil resistance (Figure 2G), which is closely related to the ionic strength,[36] also decreased significantly in the experiments with ferrihydrite addition (i.e., S+Fe and S+Fe +B), compared to the experiments without ferrihydrite (i.e., S and S+B). This trend could be attributed to three factors: (1) the Fe(III) mineral released iron ions into the soil under the action of microorganisms; (2) the enhanced Fe(III) reduction accelerated the microbial consumption of organics accompanied by the release of ions (such as organic acid and $NH_4^+$);[31] and (3) the synthesis of potential conductive minerals (typically, magnetite) due to the reduction of Fe(III).[40,41]

Overall, our results suggest that the addition of electroactive microbes significantly enhances the biogeochemical cycling of soil organic matter and Fe(III) minerals, leading to decreases in TOC, TN, and pH, increases in Fe(II) concentration, and more negative $\zeta$ potential in soil. On the other hand, the addition of ferrihydrite, representing Fe-rich soil, provided more surface area for the adsorption of ions and microbes, therefore resulting in smaller increases in soil conductivity from the exogenous electroactive microbes and a decrease in soil resistance.

**Microbial Community Diversity in Response to Electroactive-Microbes Enhanced Fe(III) Mineral Reduction in Soil.** High-throughput sequencing indicated that the bacterial community in natural soil varied markedly with the addition of exogenous ferrihydrite and electroactive microbes. As shown in Figure 3A−D, the top five bacterial phyla in natural soil alone (Figure 3A) were *Firmicutes* (39.66%), *Proteobacteria* (19.60%), *Bacteroidota* (18.99%), *Actinobacteriota* (8.76%), and *Chloroflexi* (5.28%), consistent with previous research on farmland soil.[42] Other phyla, such as *Planctomycetota*, *Halanaerobiaeota*, *Elusimicrobiota*, and *Verrucomicrobiota*, were also detected. The addition of either ferrihydrite or electroactive microbes, or both, into soil increased the abundance of *Proteobacteria* from 19.60% to 33.44%, 35.04%, and 39.99%, respectively. The increase of *Proteobacteria* in the experiments with exogenous electroactive microbes (i.e., S+B and S+Fe+B) can be attributed to the presence of *Shewanella* sp. and *Geobacter* sp., which are both electroactive microbes and major components of the bacterial phyla of *Proteobacteria*.[43]

Compared to the experiment with only electroactive microbes (S+B), the additional ferrihydrite amendment (S +Fe+B) further increased the *Proteobacteria* abundance by 5%. This indicates that Fe-rich soil can further trigger the growth of these microbes. Similar to *Proteobacteria*, the abundance of *Cyanobacteria* also increased from 0.06% in the experiment with soil only to 18.07%, 11.16%, and 4.30% with the addition of ferrihydrite, electroactive microbes, or both, respectively. Whereas the increased fraction of *Cyanobacteria* with the addition of electroactive microbes might result from increased $CO_2$ generated from enhanced degradation of organic matter, the addition of ferrihydrite stimulated the growth of *Cyanobacteria* because it satisfied the demand for Fe in photosynthesis and fixation of $N_2$.[44] The role of *Cyanobacteria* in $N_2$ fixation could explain part of the increase in TN (in addition to ammoniation of nitrogenous organics) in S+Fe. Noticeably, the decrease in *Cyanobacteria* abundance in S+Fe +B relative to S+B and S+Fe may be due to the loss of *Cyanobacteria* in competition with more diverse microbes.

In contrast to *Proteobacteria* and *Cyanobacteria*, the abundance of *Firmicutes* decreased with the addition of ferrihydrite or electroactive microbes. Less abundant *Firmicutes* in these experiments can be explained by the loss of *Firmicutes*' advantage in competition with *Proteobacteria*. Decreases in *Firmicutes* under such conditions was also observed in previous studies.[45] Along with changes in the abundance of specific phyla, the total number of microbial species also changed in response to the addition of ferrihydrite or electroactive microbes. In the experiment with soil only (S), the total number of species was 739, and this number decreased to 716 in the experiment with both ferrihydrite and electroactive microbes (S+Fe+B) and further decreased to 466 in the experiment with exogenous electroactive microbes (S+B). In the experiment with only ferrihydrite addition (S+Fe), 415 species were detected (Figure 3E). Consistently, a decrease of the microbial community richness indexes (Ace, Chao) has also been observed in response to exogenous Fe(III) minerals or electroactive microbes (Table S1). Furthermore, the PLS-DA score map in the phylum levels showed a large degree of separation among the four experiments, indicating that the different treatments caused significant differentiation of the microbial communities (Figure 3F). These results suggest that the soil microbial community became less diverse in response to the exogenous sources, while the coupling of electroactive bacteria and Fe(III) minerals led to a rebound in species numbers. The diversity of microbial communities in S+Fe+B may be due to the enhanced Fe reduction providing the carbon source for more microorganisms (by accelerating the turnover of organics) and establishing electron transport chains between electroactive bacteria and other microflora.

**Electroactive Microbes Impact Other Biogeochemical Cycles in Soil that are Related to Fe(III)-Mineral Transformation.** Correlations between several microbes at the genus and phylum levels were found in the experiment with the addition of both ferrihydrite and microbes (S+Fe+B, Figure 4). The first groups of microbes that showed strong positive correlation are *Halanerobiaeota*, *Firmicutes*, *Firobacterota*, *Sumerlaeota*, and *Armatimonadota*. These species are


https://doi.org/10.1021/acs.est.3c00407
Environ. Sci. Technol. 2023, 57, 7743−7752

known for the degradation of cellulose and lignin and are abundant in saline-alkali soils.[46−48] The coexistence of *Firobacterota* and *Armatimonadota* was also found in previous studies of rhizosphere loam soil (pH 5.6, with 2% total carbon).[49] The second group of microbes that are positively correlated are those capable of methanogenesis (*Gemmatimonadota*), N transformation, and Fe(III) reduction (*Acidobacteriota*, *Proteobacteria*). The microbial differentiation and the coexistence of N transformation and Fe(III) reduction functions can also be observed at the genus level (Figure 4A and Figure S3), where a positive correlation was observed between *Alkaliphilus*, *unclassified_c_Clostridia*, *Anaerosolibacter*, *Thermincola*, *Dethiobacter*, and *Armatimonadota*.[50] As a result, the highest OTU number of putative functions related to C conversion (up to 53702) and N conversion (up to 33128) occurred in S+Fe+B among all groups, indicating the accelerated carbon and nitrogen turnover driven by the enhanced microbial Fe(III) reduction (Figure S4).

The coexistence of these microbes indicates that the addition of electroactive microbes influences not only Fe(III)-mineral reduction in soil but also other metabolic reactions (Figure S5). For example, the Fe(II) produced from the Fe(III)-mineral reduction can be utilized by the nitrate-dependent Fe(II)-oxidizers. Moreover, the genetic data point to that the coexistence of methanogens and Fe(III) reducers is achieved by interspecies electron transfer, as the enrichment of exoelectrogens (e.g., *Geobacter*) and hydrogenotrophic methanogens (e.g., *Gemmatimonadota*) increased with the addition of both ferrihydrite and microbes (S+Fe+B). Similar phenomenon of increased rates of methane production after the amendment of microorganisms involved in interspecies electron transfer were also reported in previous studies.[51−53] Such electron transfer requires redox-active compounds to form a network between the different species.[18,40,54] In our system, this compound can be organic matter or potentially magnetite formed by the reduction of Fe(III) minerals as shown in Figure 5.[55−57] In natural soils, the organic matter (typically, humus) performing MIET (mediated interspecific electron transfer) is abundant, while the conductive minerals involved in DIET (direct interspecific electron transfer) with a higher electron transfer efficiency are relatively poor. So, the electroactive bacteria performing dissimilatory iron reduction to synthesize magnetite show the potential in strengthening DIET in soil ecosystems. Bioproduction of magnetite by either *Geobacter* or *Clostridia*, *Anaerosolibacter*, and *Thermincola* shown in our soil systems has been demonstrated.[41,58] As shown in a previous study on bioelectrochemistry,[45] the combination of exogenous magnetite with electrodes builds an extracellular electron transfer network in soil, strengthening the direct interspecific electron transfer and long-distance electron transport.

In conclusion, we observed that the addition of electroactive microbes into soil significantly changes its geochemical properties and the microbial community compositions, regardless the content of ferrihydrite in soil. Specifically, exogenous electroactive microbes decreased the soil pH, TOC, and TN but increased the soil conductivity and promoted Fe(III) reduction. The addition of electroactive microbes also changed the soil microbial community from *Firmicutes*-dominated to *Proteobacteria*-dominated, while the total number of species in the soil decreased from over 700 to less than 500. Moreover, the coexistence of N-transforming bacteria, Fe(III)-reducing bacteria, and methanogens was observed with the addition of electroactive microbes in Fe-rich soil (experiment S+Fe+B), indicating interspecies electron transfer (directly or indirectly) and the impact of enhanced Fe(III) reduction by electroactive-microbes on other biogeochemical processes, such as greenhouse gas emission and N preservation and loss from soil (Figure 6). Additionally, the application amount of exogenous electroactive microbes needs to be considered in site studies, which may bring disasters to the structure and function of soil microbial communities if they exceed the carrying capacity of soil ecosystems.

## ■ ASSOCIATED CONTENT

### Supporting Information

The Supporting Information is available free of charge at https://pubs.acs.org/doi/10.1021/acs.est.3c00407.

Discussions of operation details of SEM, XRD, FTIR and Raman spectroscopy and visual analysis of microbial sequences, figures of XRD spectra of Fe minerals in original soil, microbial composition of the cultures enriched from the three-electrode bioelectrochemical system, phylogenetic analysis based on the identification of microbial communities in different treatment groups, OTU number of putative functions performed by FAPROTAX related to C conversion and N conversion in different treatment groups, and clustering map of microbes by function on genus level, and tables of microbial $\alpha$-diversity indexes of different treatment groups (PDF)

## ■ AUTHOR INFORMATION


### Corresponding Authors

**Qixing Zhou** − *MOE Key Laboratory of Pollution Processes and Environmental Criteria/Tianjin Key Laboratory of Environmental Remediation and Pollution Control, College of Environmental Science and Engineering, Nankai University, Tianjin 300350, China;* orcid.org/0000-0003-4864-1715; Phone: (86)22-58890402; Email: zhouqx523@126.com; Fax: (86)22-23501117

**Tian Li** − *MOE Key Laboratory of Pollution Processes and Environmental Criteria/Tianjin Key Laboratory of Environmental Remediation and Pollution Control, College of Environmental Science and Engineering, Nankai University, Tianjin 300350, China;* orcid.org/0000-0002-8707-0348; Email: tianli1@nankai.edu.cn

### Authors

**Xiaolin Zhang** − *MOE Key Laboratory of Pollution Processes and Environmental Criteria/Tianjin Key Laboratory of Environmental Remediation and Pollution Control, College of Environmental Science and Engineering, Nankai University, Tianjin 300350, China;* orcid.org/0000-0001-8529-0155

**Yuxia Liu** − *State Key Laboratory of Petroleum Pollution Control, State Key Laboratory of Heavy Oil Processing, Department of Chemical Engineering and Environment, China University of Petroleum-Beijing, Beijing 102200, China*

**Yuge Bai** − *Department of Earth and Atmospheric Sciences, University of Alberta, Edmonton, Alberta T6G 2E3, Canada;* orcid.org/0009-0007-7331-5395

**Ruixiang Li** − *MOE Key Laboratory of Pollution Processes and Environmental Criteria/Tianjin Key Laboratory of*




https://doi.org/10.1021/acs.est.3c00407
Environ. Sci. Technol. 2023, 57, 7743−7752

*Environmental Remediation and Pollution Control, College of Environmental Science and Engineering, Nankai University, Tianjin 300350, China*

**Jintian Li** − *Institute of Ecological Science and Guangdong Provincial Key Laboratory of Biotechnology for Plant Development, School of Life Sciences, South China Normal University, Guangzhou 510631, China;* orcid.org/0000-0002-0848-5730

**Daniel S. Alessi** − *Department of Earth and Atmospheric Sciences, University of Alberta, Edmonton, Alberta T6G 2E3, Canada;* orcid.org/0000-0002-8360-8251

**Kurt O. Konhauser** − *Department of Earth and Atmospheric Sciences, University of Alberta, Edmonton, Alberta T6G 2E3, Canada*

Complete contact information is available at: https://pubs.acs.org/10.1021/acs.est.3c00407

### Author Contributions

[⊥]X.Z. and Y.L. contributed equally to this work.

### Notes

The authors declare no competing financial interest.

## ■ ACKNOWLEDGMENTS

This work was financially supported by the National Natural Science Foundation of China (U1906222 and 42007336), National Key R&D project of China (2019YFC1804104), the National Natural Science Foundation of China as a young scholar project (52100189), the Fundamental Research Funds for the Central Universities and the Ministry of Education of China (T2017002) and the Tianjin Research Innovation Project for Postgraduate Students (2022BKY010).

## ■ REFERENCES

(1) Logan, B. E.; Rossi, R.; Ragab, A.; Saikaly, P. E. Electroactive microorganisms in bioelectrochemical systems. *Nat. Rev. Microbiol.* **2019**, *17*, 307−319.

(2) von Canstein, H.; Ogawa, J.; Shimizu, S.; Lloyd, J. R. Secretion of flavins by *Shewanella* species and their role in extracellular electron transfer. *Appl. Environ. Microb.* **2008**, *74*, 615−623.

(3) Li, X. M.; Liu, L.; Liu, T. X.; Yuan, T.; Zhang, W.; Li, F. B.; Zhou, S. G.; Li, Y. T. Electron transfer capacity dependence of quinone-mediated Fe(III) reduction and current generation by *Klebsiella pneumoniae* L17. *Chemosphere* **2013**, *92*, 218−224.

(4) Xu, S.; Jangir, Y.; El-Naggar, M. Y. Disentangling the roles of free and cytochrome-bound flavins in extracellular electron transport from *Shewanella oneidensis* MR-1. *Electrochim. Acta* **2016**, *198*, 49−55.

(5) Bai, Y. G.; Sun, T. R.; Angenent, L. T.; Haderlein, S. B.; Kappler, A. Electron hopping enables rapid electron transfer between quinone-/hydroquinone-containing organic molecules in microbial iron(III) mineral reduction. *Environ. Sci. Technol.* **2020**, *54*, 10646−10653.

(6) Bretschger, O.; Obraztsova, A.; Sturm, C. A.; Chang, I. S.; Gorby, Y. A.; Reed, S. B.; Culley, D. E.; Reardon, C. L.; Barua, S.; Romine, M. F.; Zhou, J.; Beliaev, A. S.; Bouhenni, R.; Saffarini, D.; Mansfeld, F.; Kim, B. H.; Fredrickson, J. K.; Nealson, K. H. Current production and metal oxide reduction by *Shewanella oneidensis* MR-1 wild type and mutants. *Appl. Environ. Microb.* **2007**, *73*, 7003−7012.

(7) Wang, X.; Cai, Z.; Zhou, Q. X.; Zhang, Z. N.; Chen, C. H. Bioelectrochemical stimulation of petroleum hydrocarbon degradation in saline soil using U-tube microbial fuel cells. *Biotechnol. Bioeng.* **2012**, *109*, 426−433.

(8) Zhou, Q.; Li, D.; Wang, T.; Hu, X. Leaching of graphene oxide nanosheets in simulated soil and their influences on microbial communities. *J. Hazard. Mater.* **2021**, *404*, 124046.

(9) ter Heijne, A.; Pereira, M. A.; Pereira, J.; Sleutels, T. Electron storage in electroactive biofilms. *Trends Biotechnol.* **2021**, *39*, 34−42.

(10) Li, T.; Zhou, Q. X. The key role of *Geobacter* in regulating emissions and biogeochemical cycling of soil-derived greenhouse gases. *Environ. Pollut.* **2020**, *266*, 115135.

(11) Logan, B. E.; Rabaey, K. Conversion of wastes into bioelectricity and chemicals by using microbial electrochemical technologies. *Science* **2012**, *337*, 686−690.

(12) Zhou, Q.; Huang, G. *Environmental biogeochemistry and global environmental changes*; Science Press: Beijing, China, 2001.

(13) Lovley, D. R.; Holmes, D. E.; Nevin, K. P. Dissimilatory Fe(III) and Mn(IV) reduction. *Adv. Microb. Physiol.* **2004**, *49*, 219−286.

(14) Cornell, R. M.; Schwertmann, U. *The iron oxides: structure, properties, reactions, occurrences, and uses*; Wiley-vch, Weinheim, Germany, 2003.

(15) Weber, K. A.; Achenbach, L. A.; Coates, J. D. Microorganisms pumping iron: anaerobic microbial iron oxidation and reduction. *Nat. Rev. Microbiol.* **2006**, *4*, 752−764.

(16) O'Loughlin, E. J.; Gorski, C. A.; Scherer, M. M.; Boyanov, M. I.; Kemner, K. M. Effects of oxyanions, natural organic matter, and bacterial cell numbers on the bioreduction of lepidocrocite (*gamma*-FeOOH) and the formation of secondary mineralization products. *Environ. Sci. Technol.* **2010**, *44*, 4570−4576.

(17) Kappler, A.; Straub, K. L. Geomicrobiological cycling of iron. *Rev. Mineral. Geochem.* **2005**, *59*, 85−108.

(18) Borch, T.; Kretzschmar, R.; Kappler, A.; Cappellen, P. V.; Ginder-Vogel, M.; Voegelin, A.; Campbell, K. Biogeochemical redox processes and their impact on contaminant dynamics. *Environ. Sci. Technol.* **2010**, *44*, 15−23.

(19) Canfield, D. E. Factors influencing organic carbon preservation in marine sediments. *Chem. Geol.* **1994**, *114*, 315−329.

(20) Muehe, E. M.; Morin, G.; Scheer, L.; Pape, P. L.; Esteve, I.; Daus, B.; Kappler, A. Arsenic(V) Incorporation in vivianite during microbial reduction of arsenic(V)-bearing biogenic Fe(III) (oxyhydr)oxides. *Environ. Sci. Technol.* **2016**, *50*, 2281−2291.

(21) Sundman, A.; Vitzthum, A. L.; Adaktylos-Surber, K.; Figueroa, A. I.; van der Laan, G.; Daus, B.; Kappler, A.; Byrne, J. M. Effect of Fe-metabolizing bacteria and humic substances on magnetite nanoparticle reactivity towards arsenic and chromium. *J. Hazard. Mater.* **2020**, *384*, 121450.

(22) Zhou, Q. X.; Li, R. X.; Zhang, X. L.; Li, T. Innovative cost-effective nano-$NiCo_2O_4$ cathode catalysts for oxygen reduction in air-cathode microbial electrochemical systems. *Int. J. Env. Res. Pub. He.* **2022**, *19*, 11609.

(23) Zhou, Q. X.; Wang, S. M.; Liu, J. Q.; Hu, X. G.; Liu, Y. X.; He, Y. Q.; He, X.; Wu, X. T. Geological evolution of offshore pollution and its long-term potential impacts on marine ecosystems. *Geosci. Front.* **2022**, *13*, 101427.

(24) Lovley, D. R.; Ueki, T.; Zhang, T.; Malvankar, N. S.; Shrestha, P. M.; Flanagan, K. A.; Aklujkar, M.; Butler, J. E.; Giloteaux, L.; Rotaru, A. E.; Holmes, D. E.; Franks, A. E.; Orellana, R.; Risso, C.; Nevin, K. P. *Geobacter*: The microbe electric's physiology, ecology, and practical applications. *Adv. Microb. Physiol.* **2011**, *59*, 1−100.

(25) Zhang, X. L.; Miao, X. X.; Li, J. D.; Li, Z. Q. Evaluation of electricity production from Fenton oxidation pretreated sludge using a two-chamber microbial fuel cell. *Chem. Eng. J.* **2019**, *361*, 599−608.

(26) Li, T.; Wang, X.; Zhou, Q. X.; Liao, C. M.; Zhou, L.; Wan, L. L.; An, J. K.; Du, Q.; Li, N.; Ren, Z. Y. J. Swift acid rain sensing by synergistic rhizospheric bioelectrochemical responses. *Acs Sens.* **2018**, *3*, 1424−1430.

(27) Goldberg, S.; Johnston, C. T. Mechanisms of arsenic adsorption on amorphous oxides evaluated using macroscopic measurements, vibrational spectroscopy, and surface complexation modeling. *J. Colloid Interface Sci.* **2001**, *234*, 204−216.

(28) Vargas-Munoz, M. A.; Danchana, K.; Cerda, V.; Palacio, E. Field-deployable method for iron analysis using a simple preconcentration procedure and a 3D portable spectrophotometric system. *Microchem. J.* **2021**, *170*, 106774.

(29) Srinivasan, V. N.; Butler, C. S. Ecological and transcriptional responses of anode-respiring communities to nitrate in a microbial fuel Cell. *Environ. Sci. Technol.* **2017**, *51*, 5334−5342.
(30) Schimel, J. P.; Bennett, J. Nitrogen mineralization: Challenges of a changing paradigm. *Ecology* **2004**, *85*, 591−602.
(31) Lu, L.; Huggins, T.; Jin, S.; Zuo, Y.; Ren, Z. J. Microbial metabolism and community structure in response to bioelectrochemically enhanced remediation of petroleum hydrocarbon-contaminated soil. *Environ. Sci. Technol.* **2014**, *48*, 4021−9.
(32) Sun, T.; Guzman, J. J. L.; Seward, J. D.; Enders, A.; Yavitt, J. B.; Lehmann, J.; Angenent, L. T. Suppressing peatland methane production by electron snorkeling through pyrogenic carbon in controlled laboratory incubations. *Nat. Commun.* **2021**, *12*, 4119.
(33) Zhang, X.; Li, X.; Zhao, X.; Chen, X.; Zhou, B.; Weng, L.; Li, Y. Bioelectric field accelerates the conversion of carbon and nitrogen in soil bioelectrochemical systems. *J. Hazard. Mater.* **2020**, *388*, 121790.
(34) Limbach, L. K.; Wick, P.; Manser, P.; Grass, R. N.; Bruinink, A.; Stark, W. J. Exposure of engineered nanoparticles to human lung epithelial cells: Influence of chemical composition and catalytic activity on oxidative stress. *Environ. Sci. Technol.* **2007**, *41*, 4158−4163.
(35) Gorski, C. A.; Nurmi, J. T.; Tratnyek, P. G.; Hofstetter, T. B.; Scherer, M. M. Redox behavior of magnetite: implications for contaminant reduction. *Environ. Sci. Technol.* **2010**, *44*, 55−60.
(36) Liu, Y. X.; Alessi, D. S.; Owttrim, G. W.; Kenney, J. P. L.; Zhou, Q. X.; Lalonde, S. V.; Konhauser, K. O. Cell surface acid-base properties of the cyanobacterium *Synechococcus*: Influences of nitrogen source, growth phase and N:P ratios. *Geochim. Cosmochim. Ac.* **2016**, *187*, 179−194.
(37) Pham, D. V.; Ishiguro, M.; Tran, H. T. T.; Sato, T. Influence of phosphate sorption on dispersion of a Ferralsol. *Soil Sci. Plant Nutr.* **2014**, *60*, 356−366.
(38) Ishii, S.; Suzuki, S.; Tenney, A.; Nealson, K. H.; Bretschger, O. Comparative metatranscriptomics reveals extracellular electron transfer pathways conferring microbial adaptivity to surface redox potential changes. *Isme J.* **2018**, *12*, 2844−2863.
(39) Chen, X. D.; Han, T.; Miao, X. Y.; Zhang, X. L.; Zhao, L. X.; Sun, Y.; Ye, H. K.; Li, X. J.; Li, Y. T. Ferrihydrite enhanced the electrogenic hydrocarbon degradation in soil microbial electrochemical remediation. *Chem. Eng. J.* **2022**, *446*, 136901.
(40) Kappler, A.; Bryce, C.; Mansor, M.; Lueder, U.; Byrne, J. M.; Swanner, E. D. An evolving view on biogeochemical cycling of iron. *Nat. Rev. Microbiol.* **2021**, *19*, 360−374.
(41) Byrne, J. M.; Telling, N. D.; Coker, V. S.; Pattrick, R. A. D.; van der Laan, G.; Arenholz, E.; Tuna, F.; Lloyd, J. R. Control of nanoparticle size, reactivity and magnetic properties during the bioproduction of magnetite by *Geobacter sulfurreducens*. *Nanotechnology* **2011**, *22*, 455709.
(42) Liu, J. L.; Li, S. Q.; Yue, S. C.; Tian, J. Q.; Chen, H.; Jiang, H. B.; Siddique, K. H. M.; Zhan, A.; Fang, Q. X.; Yu, Q. Soil microbial community and network changes after long-term use of plastic mulch and nitrogen fertilization on semiarid farmland. *Geoderma* **2021**, *396*, 115086.
(43) Yan, X. J.; Du, Q.; Mu, Q. H.; Tian, L. L.; Wan, Y. X.; Liao, C. M.; Zhou, L. A.; Yan, Y. Q.; Li, N.; Logan, B. E.; Wang, X. Long-term succession shows interspecies competition of *Geobacter* in exoelectrogenic biofilms. *Environ. Sci. Technol.* **2021**, *55*, 14928−14937.
(44) Berman-Frank, I.; Quigg, A.; Finkel, Z. V.; Irwin, A. J.; Haramaty, L. Nitrogen-fixation strategies and Fe requirements in cyanobacteria. *Limnol. Oceanogr.* **2007**, *52*, 2260−2269.
(45) Zhang, X. L.; Li, R. X.; Wang, J. N.; Liao, C. M.; Zhou, L. A.; An, J. K.; Li, T.; Wang, X.; Zhou, Q. X. Construction of conductive network using magnetite to enhance microflora interaction and petroleum hydrocarbons removal in plant-rhizosphere microbial electrochemical system. *Chem. Eng. J.* **2022**, *433*, 133600.
(46) Blifernez-Klassen, O.; Klassen, V.; Doebbe, A.; Kersting, K.; Grimm, P.; Wobbe, L.; Kruse, O. Cellulose degradation and assimilation by the unicellular phototrophic eukaryote *Chlamydomonas reinhardtii*. *Nat. Commun.* **2012**, *3*, 1214.
(47) Fang, Y.; Yuan, Y.; Liu, J.; Wu, G.; Yang, J.; Hua, Z. S.; Han, J. B.; Zhang, X. Y.; Li, W. J.; Jiang, H. C. Casting light on the adaptation mechanisms and evolutionary history of the widespread sumerlaeota. *mBio.* **2021**, *12*, No. e00350-21.
(48) Wang, Y. L.; Liu, X. B. Sulfur-oxidizing bacteria involved in the blackening of basalt sculptures of the Leizhou Stone Dog. *Int. Biodeter. Biodegr.* **2021**, *159*, 105207.
(49) Nuccio, E. E.; Starr, E.; Karaoz, U.; Brodie, E. L.; Zhou, J. Z.; Tringe, S. G.; Malmstrom, R. R.; Woyke, T.; Banfield, J. F.; Firestone, M. K.; Pett-Ridge, J. Niche differentiation is spatially and temporally regulated in the rhizosphere. *Isme J.* **2020**, *14*, 999−1014.
(50) Zavarzina, D. G.; Gavrilov, S. N.; Zhilina, T. N. Direct Fe(III) reduction from synthetic ferrihydrite by haloalkaliphilic *Lithotrophic Sulfidogens*. *Microbiology* **2018**, *87*, 164−172.
(51) Liu, F. H.; Rotaru, A. E.; Shrestha, P. M.; Malvankar, N. S.; Nevin, K. P.; Lovley, D. R. Promoting direct interspecies electron transfer with activated carbon. *Energy Environ. Sci.* **2012**, *5*, 8982−8989.
(52) Lee, J. Y.; Lee, S. H.; Park, H. D. Enrichment of specific electroactive microorganisms and enhancement of methane production by adding granular activated carbon in anaerobic reactors. *Bioresour. Technol.* **2016**, *205*, 205−212.
(53) Lei, Z.; Zhang, S. X.; Wang, L. X.; Li, Q.; Li, Y. Y.; Wang, X. C.; Chen, R. Biochar enhances the biotransformation of organic micropollutants (OMPs) in an anaerobic membrane bioreactor treating sewage. *Water Res.* **2022**, *223*, 118974.
(54) Boyd, P. W.; Ellwood, M. J. The biogeochemical cycle of iron in the ocean. *Nat. Geosci.* **2010**, *3*, 675−682.
(55) Qu, X. F.; Yao, Q. Z.; Zhou, G. T.; Fu, S. Q.; Huang, J. L. Formation of hollow magnetite microspheres and their evolution into durian-like architectures. *J. Phys. Chem. C* **2010**, *114*, 8734−8740.
(56) Xiong, Y.; Ye, J.; Gu, X. Y.; Chen, Q. W. Synthesis and assembly of magnetite nanocubes into flux-closure rings. *J. Phys. Chem. C* **2007**, *111*, 6998−7003.
(57) Tian, L. L.; Song, J. T.; Ren, Y. Y.; Zhao, Q.; Li, Y.; Luo, X.; Li, N.; Li, T.; Wang, X. Biosynthesis and recycling of magnetite nanocatalysts from Fe-rich sludge. *Resour. Conserv. Recycl.* **2022**, *182*, 106348.
(58) Lovley, D. R.; Stolz, J. F.; Nord, G. L.; Phillips, E. J. Anaerobic production of magnetite by a dissimilatory iron-reducing microorganism. *Nature* **1987**, *330*, 252−254.


https://doi.org/10.1021/acs.est.3c00407
*Environ. Sci. Technol.* 2023, 57, 7743−7752